IIETA International Information and Engineering Technology Association
Advancing the World of Information and Engineering

Mathematical Modelling of Engineering Problems
Vol. 13, No. 2, February, 2026, pp. 313-320
Journal homepage: http://iieta.org/journals/mmep

Adaptive Data Rate Enhancement for Long Range Wide Area Network with Dynamic Margin

Hamid Azwar[1,2], Ansar Jamil[1*], Zuhairiah Zainal Abidin[1]

[1] Faculty of Electrical and Electronic Engineering, Universiti Tun Hussein Onn Malaysia, Parit Raja 86400, Malaysia
[2] Program Studi Teknik Elektronika Telekomunikasi, Politeknik Caltex Riau, Pekanbaru 28265, Indonesia

Corresponding Author Email: ansar@uthm.edu.my

https://doi.org/10.18280/mmep.130208

Received: 18 November 2025
Revised: 16 January 2026
Accepted: 24 January 2026
Available online: 15 March 2026

Keywords:
Adaptive Data Rate, Dynamic Margin, Signal-to-Noise Ratio variability, packet delivery, shadowing, energy efficiency

ABSTRACT

The standard Adaptive Data Rate (ADR) mechanism in Long Range Wide Area Network (LoRaWAN) employs a static safety margin, which frequently results in packet loss caused by collisions and energy waste in dense, time-varying environments. To address this limitation, this paper proposes the Dynamic Margin ADR (DM-ADR) algorithm. This method adaptively determines the optimal safety margin based on the standard deviation derived from the twenty most recent uplink Signal-to-Noise Ratio (SNR) samples. We evaluated the performance of DM-ADR against the standard ADR baseline using the Network Simulator 3 (NS-3) network simulator under diverse shadowing conditions and node densities. Simulation results demonstrate that the proposed method significantly enhances both network reliability and energy efficiency. Specifically, in a dense network comprising 700 nodes, DM-ADR improved the packet delivery ratio (PDR) by 23.10 percentage points and reduced average energy consumption by approximately 52%. Furthermore, under severe channel variability (σ = 6), the algorithm maintained its robustness, achieving a PDR improvement of 37.93 percentage points compared to the baseline. These findings indicate that Dynamic Margin adaptation offers a scalable and energy-efficient solution for massive LoRaWAN deployments.

1. INTRODUCTION

Long Range Wide Area Network (LoRaWAN) is widely recognized as a leading solution within the Low Power Wide Area Network (LPWAN) landscape, offering a scalable and energy-efficient framework for long-range communication [1, 2]. However, in dense network scenarios, its performance is often compromised by high contention and stochastic channel variations, which lead to reduced packet delivery ratios (PDRs) and increased energy consumption [3, 4].

The performance and longevity of LoRaWAN devices are fundamentally governed by transmission parameters. Key among these is the Spreading Factor (SF), which defines the chips-per-symbol ratio, effectively balancing data throughput against signal robustness. Transmission Power (TP) dictates signal intensity, directly influencing both coverage range and energy consumption. Furthermore, Bandwidth (BW) determines channel capacity and data rate, while the Coding Rate (CR) enhances error correction capabilities to mitigate interference. Therefore, the optimal configuration of these parameters is critical to achieving a balanced trade-off between communication range, reliability, and energy efficiency [5-7].

The dynamic optimization of transmission parameters based on Channel State Information (CSI) has become a primary focus in various modern wireless communication systems [8]. However, in the context of LoRaWAN, the standard Adaptive Data Rate (ADR) mechanism often relies on static parameters that fail to adapt to rapid channel fluctuations. The LoRaWAN specification defines the ADR mechanism to optimize transmission parameters. While standard ADR implementations demonstrate robustness in stable environments, they suffer from a critical rigidity due to the use of a fixed 10 dB safety margin, which often leads to suboptimal resource allocation in dynamic conditions [9, 10]. This reliance on a static margin creates a fundamental trade-off that standard ADR fails to resolve.

In stable channel conditions, the fixed 10 dB margin is often excessively conservative, compelling devices to utilize higher SF or TP than required, which results in unnecessary energy consumption and airtime wastage [11]. Conversely, in volatile channels prone to bursty interference or shadowing, this fixed margin may prove inadequate, leading to link instability and significant packet loss [12]. Consequently, the lack of an adaptive safety margin mechanism in standard ADR constitutes a critical deficiency in optimizing dense, stationary LoRaWAN deployments.

In this context, this paper proposes the Dynamic Margin Adaptive Data Rate (DM-ADR). This mechanism replaces the fixed safety margin with a bounded dynamic margin derived directly from the standard deviation of recent uplink Signal-to-Noise Ratio (SNR) samples. This approach allows the network server to explicitly capture fluctuations caused by the environment by expanding the margin during volatile periods

to prevent packet loss and reducing it during stable periods to conserve energy. We implemented DM-ADR in the Network Simulator 3 (NS-3) network simulator and evaluated it against standard ADR and representative schemes. The results demonstrate that alignment of the safety margin with observed SNR variability significantly improves the trade-off between reliability and energy efficiency in large-scale deployments.

The remainder of this paper is organized as follows: Section 2 reviews the related work, while Section 3 provides an overview of the standard ADR in LoRaWAN. Section 4 details the proposed DM-ADR method, followed by the description of the simulation configuration in Section 5. Section 6 presents the results and discussion, and Section 7 concludes the paper and outlines future work.

2. RELATED WORK

Several enhancements have been proposed to improve ADR stability by refining how the network estimates channel quality. Many of these approaches, such as ADR+ [11], ADRmin [13], and G-ADR [14], primarily modify the SNR processing stage. For instance, ADR+ replaces the maximum SNR with an average value, while lightweight variants like ADR Lite [15] add control factors to balance reliability and energy consumption. Although these modifications can successfully reduce parameter oscillations and improve convergence behavior, the majority of existing schemes still retain the conventional assumption of a fixed safety margin. This margin is typically set as a constant value applied uniformly across time and devices, regardless of actual channel conditions. As a result, even with improved SNR estimation, the underlying link budget decision remains constrained by a static margin that does not explicitly adapt to the time-varying uncertainty of the channel. This rigidity can limit performance gains in dense networks characterized by fluctuating interference and stochastic propagation [16].

The limitations associated with using a static margin, which often result in energy waste on stable links or connectivity loss on poor links, have driven the development of dynamic margin adaptation methods. To address this issue, de Jesus et al. [17] proposed ADRx. This algorithm automatically tunes the link margin at runtime based on a target Data Extraction Rate (DER) without requiring prior network knowledge. The mechanism operates reactively by increasing the margin by 5 dB if reliability falls below the target to restore connectivity and decreases it by 2.5 dB if performance exceeds expectations. Meanwhile, specifically for mobile scenarios, Wang et al. [18] introduced the mobile ADR algorithm. This method dynamically calculates the margin based on physical parameters rather than a fixed constant. By integrating the distance of the node to the gateway, the movement speed, and the trend of SNR fluctuations, this approach successfully improves DER values and reduces energy consumption in variable environments.

Despite these advancements, there remains a distinct lack of a server-side mechanism with low complexity designed specifically for stationary nodes that adapts the safety margin explicitly based on environmental signal volatility. Existing dynamic methods often rely on reactive packet loss metrics, which may introduce latency or require complex mobility parameters that are unnecessary for static deployments. This paper addresses this gap by proposing a statistical approach that aligns the safety margin directly with the observed channel variance to optimize the trade off between reliability and energy efficiency.

3. STANDARD ADAPTIVE DATA RATE

LoRaWAN is a standard LPWAN protocol designed to support long-range communication with low power consumption for IoT applications. The network architecture operates on a star-of-stars topology composed of three main elements: end-devices, gateways, and back-end servers [19]. Unlike simple point-to-point configurations, LoRaWAN utilizes a star topology where the gateway centrally receives chirp signals, relieving sensor nodes from the burden of routing processes. This architecture not only ensures superior energy efficiency but also facilitates end-to-end data security mechanisms (such as Advanced Encryption Standard (AES)) and centralized network management using platforms like Chirpstack, making it an ideal standard for disaster mitigation in remote regions [20].

The physical layer of LoRaWAN utilizes LoRa modulation, a proprietary spread spectrum technology developed by Semtech [21]. The performance of a LoRa link is governed by critical transmission parameters, primarily the SF, TP, and BW. The SF ranges from 7 to 12, while TP typically varies between 2 dBm and 14 dBm. There is an inherent trade-off in configuring these parameters: utilizing a high SF and high TP extends the transmission range up to 15 km in suburban areas but results in a decreased data rate and significantly higher energy consumption. Conversely, lower SF and TP settings yield higher data rates and reduced power consumption but shorten the effective communication range [22].

ADR is a critical mechanism within the LoRaWAN protocol designed to optimize network capacity and energy efficiency by dynamically adjusting transmission parameters, primarily the SF and TP. In the standard LoRaWAN ADR mechanism, the process of adjusting the SF and TP is based on the maximum SNR value of the uplink packets received by the gateway. The network server then compares this maximum SNR value with the minimum required SNR for a specific SF, according to the sensitivity table for the LoRa module. The standard ADR algorithm can be seen in the following Algorithm 1 [11]:

Algorithm 1: Standard Adaptive Data Rate (ADR)

1: Initialize: SF [7,12], TP [2 dBm,14 dBm], Margin = 10 dB
2: SNR_{req}: demodulation floor (current data rate)
3: SNR_{max}: max (SNR of last 20 frames)
4: $SNR_{margin} = SNR_{max} - SNR_{req} - Margin$
5: $N_{step} = interger\left[SNR_{margin}/3\right]$
6: while $N_{step} > 1$ and $SF > SF_{min}$ do
7: $SF = SF - 1$
8: $N_{step} = N_{step} - 1$
9: end while
10: while $N_{step} > 0$ and $TP > TP_{min}$ do
11: $TP = TP - 3$
12: $N_{step} = N_{step} - 1$
13: end while
14: while $N_{step} < 0$ and $TP < TP_{max}$ do
15: $TP = TP + 3$
16: end while
17: Output: TP and SF

SNR_{max} is the maximum value of the last 20 SNR values received by the gateway from a LoRaWAN device. This value represents the best signal quality achieved within a specific timeframe, typically during the last 20 uplink transmissions. On the other hand, the SNR requirement (SNR_{req}) is the minimum SNR value needed for a LoRa signal to be received and demodulated correctly at a specific SF. This value indicates the receiver's sensitivity threshold. The larger the SF, the lower the SNR_{req}, indicating the system is more resistant to noise but has a slower data rate. The required SNR values are usually already defined based on the results of physical LoRaWAN testing, as follows (for 125 kHz BW) in Table 1. The resulting margin is translated into an integer number of adaptation steps, $N_{step} = int[SNR_{margin}/3]$, following the ADR convention that approximately 3 dB corresponds to one control step. When N_{step} is positive, the link has excess margin, and the algorithm first increases the data rate by decrementing the SF step by step until the minimum SF is reached or the steps are exhausted. Any remaining positive steps are then applied to reduce TP in 3 dB decrements to improve energy efficiency. When N_{step} is negative, the link margin is insufficient, and the algorithm increases TP in 3 dB increments, up to TP_{max}, to restore reliability. The algorithm outputs the updated SF and TP values for subsequent transmissions.

Table 1. Required Signal-to-Noise Ratio (SNR) of each Spreading Factor (SF) [23]

SF	$SNR_{req}(dB)$
7	−7.5
8	−10
9	−12.5
10	−15
11	−17.5
12	−20

In the standard ADR mechanism in LoRaWAN, the margin value is fixed at 10 dB as part of the link budget calculation to maintain communication reliability. This margin serves as a buffer or safety factor against various conditions that can degrade signal quality, such as fading, inter-device interference, environmental variations, or differences in receiver sensitivity in the real world compared to theoretical values. In other words, even though the device's SNR is already high enough to support a certain SF, the system still reduces it by 10 dB to allow for tolerance if channel conditions suddenly worsen.

4. THE PROPOSED DYNAMIC MARGIN ADAPTIVE DATA RATE METHOD

To address the limitations of fixed-margin ADR under density-driven interference and channel variability, we propose DM-ADR, which adapts the safety margin online based on recent SNR fluctuations.

In the DM-ADR method, the dynamic margin value plays an important role as an adaptive component, replacing the fixed 10 dB margin in the standard ADR algorithm. This margin is no longer constant but rather changes according to the communication channel conditions experienced by the device. The calculation is based on the variation in the quality of the received signal, using the formula:

$$Dynamic\ Margin = SNR_{stddev} \quad (1)$$

In that formula, SNR_{stddev} is the standard deviation of the last 20 SNR values received by the gateway from a single device. Specifically, for each end device, the network server maintains a buffer containing the last 20 uplink SNR samples reported by the gateway ($N = 20$). From these samples, the server computes the mean μ and the standard deviation SNR_{stddev} as:

$$\mu = \frac{1}{N}\sum_{i=1}^{N} \mathrm{SNR}_i\,, \qquad N = 20 \quad (2)$$

$$SNR_{stddev} = \sqrt{\frac{1}{N}\sum_{i=1}^{N}(\mathrm{SNR}_i - \mu)^2}, \qquad N = 20 \quad (3)$$

This provides a lightweight yet informative estimate of short-term fluctuations, low SNR_{stddev} corresponds to stable uplink conditions, whereas high SNR_{stddev} suggests bursty interference and/or propagation uncertainty. The resulting SNR_{stddev} is used as an input to dynamically adjust the ADR safety margin. To keep the system stable, the dynamic margin value is limited to the range of 2 to 10 dB. The lower limit of 2 dB is applied to prevent the system from becoming overly sensitive to small changes in the actual stable channel, while the upper limit of 10 dB is used to prevent excessive margin growth, which would reduce energy efficiency. With these limitations, DM-ADR can adapt in a balanced way between efficiency and reliability. Overall, the DM-ADR algorithm, which is the proposed method in this study, can be seen in the following Algorithm 2:

Algorithm 2: Dynamic Margin Adaptive Data Rate (DM-ADR)

1: Initialize: SF [7,12], TP [2 dBm,14 dBm]
2: Initialize: $DM_{min} = 2, DM_{max} = 10$
3: SNR_{req}: demodulation floor (current data rate)
4: SNR_{avg}: average (SNR of last 20 frames)
5: SNR_{stddev}: Deviation of last 20 SNR frames
6: $DM = SNR_{stddev}$
7: while $DM < DM_{min}$ do
8: $DM = DM_{min}$
9: end while
10: while $DM > DM_{max}$ do
11: $DM = DM_{max}$
12: end while
13: $SNR_{margin} = SNR_{avg} - SNR_{req} - DM$
14: $N_{step} = interger[SNR_{margin}/3]$
15: while $N_{step} > 1$ and $SF > SF_{min}$ do
16: $SF = SF - 1$
17: $N_{step} = N_{step} - 1$
18: end while
19: while $N_{step} > 0$ and $TP > TP_{min}$ do
20: $TP = TP - 3$
21: $N_{step} = N_{step} - 1$
22: end while
23: while $N_{step} < 0$ and $TP < TP_{max}$ do
24: $TP = TP + 3$
25: end while
26: Output: TP and SF

DM-ADR extends the standard LoRaWAN ADR procedure by replacing the fixed safety margin with a bounded dynamic margin that reflects short-term link variability. At initialization, the end device operates within the allowed configuration ranges, with the SF constrained to 7 through 12 and the transmit power TP constrained to 2 dBm through 14 dBm. The algorithm also defines lower and upper bounds for the dynamic margin, DM_{min} set to 2 dB and DM_{max} set to 10 dB, to prevent overly aggressive or overly conservative behaviour. For each ADR update, the network server processes the most recent uplink history and computes the average SNR over the last 20 successfully received frames, denoted SNR_{avg}, together with the corresponding standard deviation SNR_{stddev}. The standard deviation is used as the dynamic margin candidate, $DM = SNR_{stddev}$, since it directly captures the short-term fluctuation level of the link. The margin is then clipped to the interval between DM_{min} and DM_{max} to ensure stability across a wide range of channel conditions. The available link budget is quantified using $SNR_{margin} = SNR_{avg} - SNR_{req} - DM$, where SNR_{req} is the demodulation threshold required by the current data rate.

5. SIMULATION CONFIGURATION

A comparative evaluation of the proposed DM-ADR against the baseline Standard ADR was conducted within a discrete-event simulation environment using NS-3. The implementation was realized through custom C++ simulation scripts built on top of the widely used LoRaWAN module for NS-3, which provides an end-to-end LoRaWAN stack (PHY, MAC, and network-side control) suitable for reproducible ADR studies. These simulations employed a standard LoRaWAN network module [24, 25].

The simulation parameters used can be seen in Table 2, which includes physical configuration aspects and MAC, as well as simulation environment parameters such as the number of devices, data transmission period, and simulation duration. All experiments were conducted in the EU868 band over a 5000 × 5000 m deployment with a single gateway and 100 to 700 end devices. Uplink traffic is generated periodically every 10 minutes using a 20-byte payload, and each run lasts 2 days to capture steady-state ADR behaviour under sustained channel contention.

Table 2. Simulation setup

Parameter	Value / Setting
Frequency Band	868 MHz
Number of End Devices	100, 300, 500, 700
Number of Gateways	1
Simulation Area	5000 × 5000 m
Transmission Power (TP)	2–14 dBm
Spreading Factor (SF)	7–12
Traffic Model	Periodic
Bandwidth (BW)	125 kHz
Coding Rate (CR)	4/5
Packet Interval	10 minutes
Payload Size (PL)	20 bytes
Duty Cycle	1%
Simulation Duration	2 days
Number of Iterations	5
Channel Model	Log-Distance with Log-Normal Shadowing
$PL(d_0)$	128.95
Path Loss Exponent (n)	2.32
Shadowing Std. Dev. (σ)	0 to 6

To validate the proposed method's adaptiveness to realistic channel variations, the simulation environment utilizes the Log-Normal Shadowing model, with parameters rigorously aligned with the benchmark study by Slabicki et al. [11]. By adopting the propagation configuration and stochastic parameters defined in this established framework, we ensure that the simulated SNR fluctuations are statistically consistent with actual field environments. This approach confirms the method's robustness against realistic channel impairments without the need for a separate physical measurement campaign. This composite model accounts for both the deterministic signal attenuation due to distance and the stochastic variations caused by obstacles in the propagation path. The path loss $PL(d)$ at a distance d from the gateway is expressed as:

$$PL(d) = PL(d_0) + 10\, n\, \log_{10}\left(\frac{d}{d_0}\right) + X_\sigma \qquad (4)$$

where, $PL(d_0)$ represents the path loss at a reference distance d_0 and n denotes the path loss exponent, which characterizes the signal decay rate specific to the environment (e.g., urban or rural). To simulate the irregularity of the wireless channel and the presence of obstacles (shadowing), a zero-mean Gaussian random variable X_σ with standard deviation σ (in dB) is introduced. The parameters are set to $n = 2.32$ and $PL(d_0) = 128.95$ [11], consistent with the log-distance formulation available in NS-3 propagation-loss modelling. Finally, to reduce randomness and improve statistical confidence, each scenario is repeated for 5 independent iterations, and the reported results are averaged across runs.

The energy consumption of LoRaWAN end devices in this study is modelled by considering the three main operational states of the radio transceiver: transmission (TX), reception (RX), and standby or sleep. The energy consumed in each state is defined as the product of the supply voltage, the current drawn, and the duration of the state, expressed as:

$$E = V \times I \times t \qquad (5)$$

where, V is the supply voltage, I is the current in amperes, and t is the duration in seconds. The total energy consumed by a

node over the course of the simulation is therefore given by:

$$E_{total} = E_{TX} + E_{RX} + E_{standby} \quad (6)$$

Transmission energy is primarily determined by the configured TP and the time-on-air (ToA) of each packet. The ToA is computed according to the LoRa physical layer parameters, specifically the SF, BW, CR, and payload size (PL). The symbol duration is defined as

$$T_{sym} = \frac{2^{SF}}{BW} \quad (7)$$

$$ToA = \left(n_{preamble} + 4.25\right) \times T_{sym} + N_{payload} \times T_{sym} \quad (8)$$

where, $n_{preamble} = 8$ (default in LoRaWAN), and $N_{payload}$ is the number of payload symbols derived from the LoRa specification. Thus, the energy consumed during transmission can be calculated as:

$$E_{TX} = V \times I_{TX} \times ToA \quad (9)$$

This formulation ensures that higher SFs (longer ToA) and higher transmit powers both result in higher energy costs, reflecting the reliability–lifetime trade-off in LoRaWAN. After each uplink, a Class A LoRaWAN end device opens two receive windows ($RX1$ and $RX2$). Even if no downlink packet is received, the device remains in reception mode, consuming a constant current for the duration of these windows. The reception energy is therefore modeled as:

$$E_{RX} = V \times I_{RX} \times \left(t_{RX1} + t_{RX2}\right) \quad (10)$$

where, I_{RX} is the current consumption in reception mode, and t_{RX1}, t_{RX2} are the durations of the two windows. When not transmitting or receiving, the device remains in standby or sleep mode, drawing a minimal current $I_{standby}$. Although this contribution is small in high-traffic scenarios, it becomes dominant when devices send packets infrequently. The standby energy is given by:

$$E_{standby} = V \times I_{standby} \times t_{standby} \quad (11)$$

At the beginning of the simulation, each device is initialized with a fixed energy budget of 10,000 J. During runtime, the simulator continuously subtracts the consumed energy from this budget according to the device state. From this, we derive the average energy consumption per device, the total energy consumed by the network, and the percentage of energy depletion. This framework allows us to evaluate the trade-offs between link reliability and energy efficiency across different ADR algorithms.

6. RESULTS AND DISCUSSION

To evaluate the reliability of uplink communication under varying network densities, we analyze the PDR for all considered ADR algorithms.

Figure 1 presents the PDR performance as the network size scales from 100 to 700 end devices under different shadowing conditions. The results reveal a significant performance divergence between the baseline and the proposed method. The Standard ADR, depicted by the dashed lines, exhibits high sensitivity to both network density and channel variability. As shown in the data, the performance of Standard ADR degrades significantly as the number of nodes increases. Moreover, it displays a wide dispersion in reliability depending on the environmental shadowing. For instance, at 700 nodes, the PDR drops to 63.81% in a static channel where $\sigma = 0$ but remains at 78.99% under higher shadowing variability where $\sigma = 2$. This large gap of approximately 15 percentage points indicates that the fixed margin mechanism fails to provide consistent reliability across diverse channel conditions. In contrast, the proposed DM-ADR demonstrates superior robustness and stability, represented by the tightly clustered solid lines. Regardless of the shadowing intensity, the performance of DM-ADR remains highly consistent with minimal variance between scenarios. Even at the highest density of 700 nodes, DM-ADR maintains a high PDR ranging from 86.91% for $\sigma = 0$ to 89.31% for $\sigma = 2$. This represents a substantial improvement over the baseline. Specifically, in the static channel scenario, DM-ADR outperforms Standard ADR by 23.10 percentage points. These results confirm that replacing the fixed margin with a dynamic calculation based on signal deviation effectively mitigates interference caused by high density while ensuring predictable network behaviour.

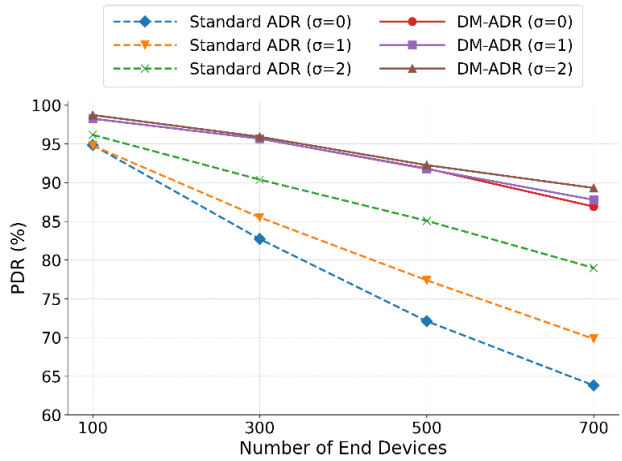

Figure 1. Packet Delivery Ratio (PDR) versus nodes for Standard Adaptive Data Rate (ADR) and Dynamic Margin ADR (DM-ADR)

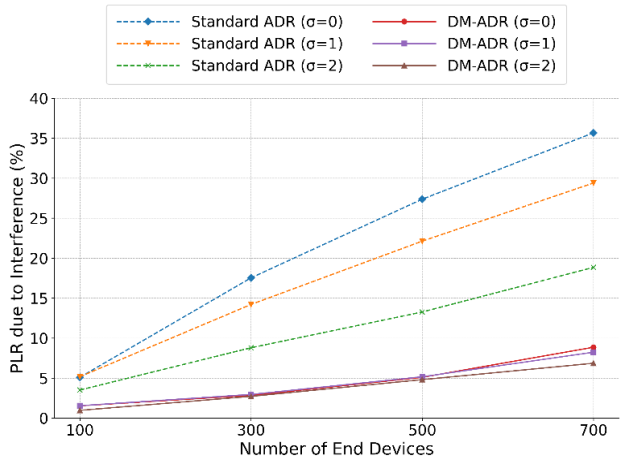

Figure 2. Packet Loss Ratio (PLR) due to interference versus nodes for Standard Adaptive Data Rate (ADR) and Dynamic Margin ADR (DM-ADR)

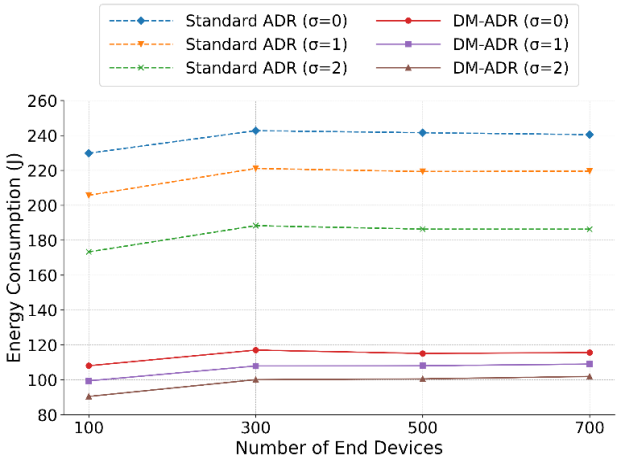

Figure 3. Energy consumption versus nodes for Standard Adaptive Data Rate (ADR) and Dynamic Margin ADR (DM-ADR)

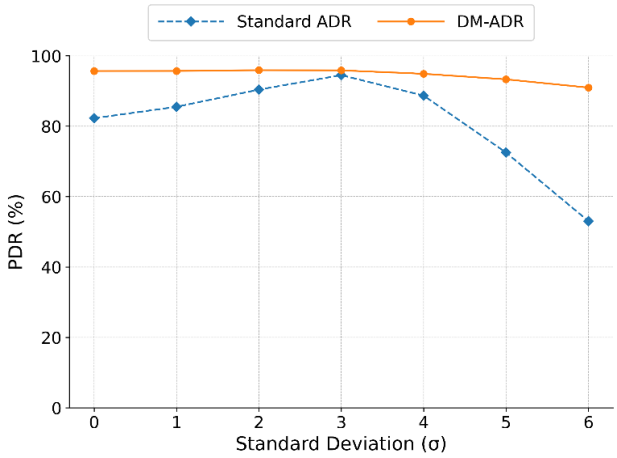

Figure 4. Packet Delivery Ratio (PDR) versus log-normal shadowing standard deviation (σ) for Standard Adaptive Data Rate (ADR) and Dynamic Margin ADR (DM-ADR)

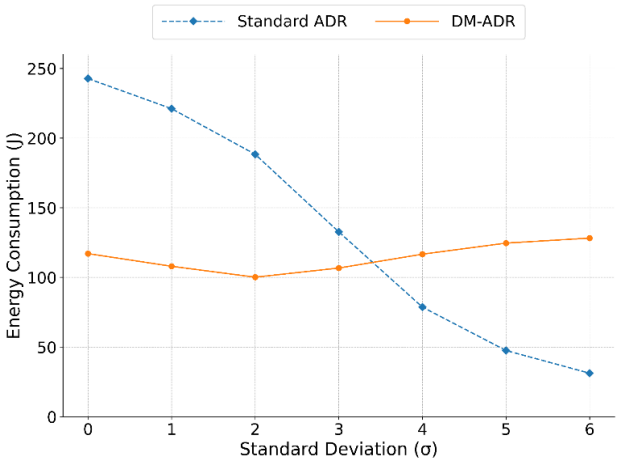

Figure 5. Energy consumption of end device versus log-normal shadowing standard deviation (σ) for Standard Adaptive Data Rate (ADR) and Dynamic Margin ADR (DM-ADR)

Packet Loss Ratio (PLR) complements PDR by measuring the percentage of transmitted uplink packets that are not successfully received at the gateway. A lower PLR indicates more reliable communication with fewer collisions and interference-related losses. Figure 2 compares the PLR performance of Standard ADR and the proposed DM-ADR under different shadowing standard deviation values (σ), representing different levels of environmental variability.

Figure 2 highlights the impact of network scale on interference loss. While both schemes show an upward trend, Standard ADR suffers from a steep increase in PLR due to its inability to cope with rising contention. Specifically, at $\sigma = 0$, the PLR of the standard protocol surges from 5.10% to 35.67% as the network grows to 700 nodes. Conversely, DM-ADR demonstrates superior resilience by keeping the interference PLR consistently below 9% across all tested scenarios. The proposed method significantly outperforms the baseline at high density, reducing the PLR by approximately 26.81 percentage points in static channels and 11.99 percentage points in environments with moderate shadowing. This confirms that the dynamic margin strategy effectively mitigates packet loss caused by density and maintains network stability even under heavy traffic loads.

Energy consumption is a critical metric for battery-limited LoRaWAN devices. Efficient adaptation minimizes energy use by reducing time on air and preventing retransmissions caused by packet loss. Figure 3 compares the average energy consumption of Standard ADR and DM-ADR across varying shadowing intensities (σ).

As shown in Figure 3, DM-ADR achieves superior energy efficiency compared to Standard ADR regardless of network size or shadowing intensity. The proposed method delivers substantial energy savings at 700 nodes, reducing consumption by 51.90% in static channels where $\sigma = 0$ and by 45.26% in variable channels where $\sigma = 2$. Similar performance gains are evident at 100 nodes, with reductions ranging from 47.76% to 52.95%. While higher shadowing variability naturally decreases energy metrics for both protocols, DM-ADR maintains a more stable profile, dropping by only 11.83% compared to the 22.53% drop observed in Standard ADR as σ shifts from 0 to 2. In summary, by mitigating the need for excessive safety margins and minimizing time on air, DM-ADR effectively reduces overall energy consumption by roughly 45% to 53% relative to the standard protocol.

To further examine how environmental variability affects reliability beyond network density, we next analyze the sensitivity of PDR to log-normal shadowing intensity. Figure 4 shows the PDR of Standard ADR and DM-ADR as a function of the shadowing standard deviation (σ) for a network size of 300 end devices, where σ captures the degree of channel fluctuation in the propagation environment.

As illustrated in Figure 4, Standard ADR exhibits high sensitivity to the shadowing standard deviation (σ). The baseline performance follows a nonlinear trend where the PDR initially rises from 82.27% at $\sigma = 0$ to a peak of 94.51% at $\sigma = 3$ but subsequently suffers a drastic reduction under severe conditions. Specifically, as variability intensifies, the PDR drops to 72.52% at $\sigma = 5$ and reaches a critical low of 53.04% at $\sigma = 6$. This rapid decline indicates that the fixed margin mechanism fails to cope with extreme channel fluctuations. In contrast, DM-ADR demonstrates exceptional stability by sustaining a PDR above 90% across the entire range of tested σ values. Even at the highest uncertainty level of $\sigma = 6$, DM-ADR maintains 90.97%, which results in a substantial performance gap of 37.93 percentage points compared to the baseline. These results confirm that adapting the margin based on short-term SNR variability significantly enhances

robustness and stabilizes reliability as channel uncertainty increases.

To explicitly quantify how environmental uncertainty affects power efficiency, we analyzed the energy consumption of end devices as a function of the log-normal shadowing standard deviation. The results of this evaluation are presented in Figure 5.

Figure 5 presents a comparative analysis of energy consumption between Standard ADR and the proposed DM-ADR across varying shadowing standard deviations. In stable channel conditions where σ ranges from 0 to 2, Standard ADR exhibits excessive energy usage, peaking at 242.73 Joules at $\sigma = 0$. This inefficiency stems from the fixed 10 dB safety margin, which forces nodes to utilize higher TP or SFs than necessary for the prevailing channel quality. In contrast, DM-ADR significantly optimizes resource utilization by dynamically reducing the margin in stable environments. Consequently, at $\sigma = 0$, the proposed method consumes only 117.08 Joules, representing a reduction of approximately 51.7% compared to the baseline. As the channel volatility increases to $\sigma = 6$, a distinct trend emerges. The energy consumption of Standard ADR drops drastically to 31.21 Joules. However, this reduction must be interpreted in conjunction with the poor reliability observed in Figure 4, where the PDR falls to 53.04%. This indicates that the low energy consumption of Standard ADR in severe shadowing is not a sign of efficiency but rather a symptom of link failure and packet loss. Conversely, DM-ADR adapts to high uncertainty by expanding the safety margin, which results in a slight increase in energy consumption to 128.21 Joules at $\sigma = 6$. This additional energy investment is critical and justified as it allows DM-ADR to sustain a PDR above 90%, thereby ensuring continuous connectivity where the standard protocol fails. Thus, DM-ADR achieves a superior trade-off by conserving energy in stable conditions while allocating necessary resources to maintain reliability in volatile scenarios.

7. CONCLUSIONS

This study presented DM-ADR, a dynamic margin adaptation scheme designed to overcome the rigidity of the fixed safety margin inherent in the Standard LoRaWAN ADR. By leveraging short-term SNR variability to adjust the link budget proactively, the proposed method balances reliability and energy efficiency in high-density scenarios. Our simulation-based evaluation using the NS-3 framework demonstrates that DM-ADR delivers significant performance gains under the conditions tested. In a dense network comprising 700 nodes, the proposed algorithm improved the PDR by up to 23.10 percentage points and reduced the average energy consumption per node by approximately 52% compared to the Standard ADR baseline. These improvements are particularly evident in environments characterized by high shadowing variability, where ($\sigma = 6$). In such scenarios, DM-ADR maintained a PDR above 90%, whereas the performance of Standard ADR degraded significantly.

Future work will focus on extending the DM-ADR framework to multi-gateway architectures and mobile LoRaWAN nodes. Additionally, we intend to validate the algorithm's performance through real-world testbed experiments to confirm its robustness under heterogeneous traffic patterns and unpredictable physical-layer impairments.

ACKNOWLEDGEMENTS

The author would like to express gratitude to the Faculty of Electrical and Electronic Engineering (FKEE) at Universiti Tun Hussein Onn Malaysia and Politeknik Caltex Riau for their full support of this research.

REFERENCES

[1] Mekki, K., Bajic, E., Chaxel, F., Meyer, F. (2019). A comparative study of LPWAN technologies for large-scale IoT deployment. ICT Express, 5(1): 1-7. https://doi.org/10.1016/j.icte.2017.12.005

[2] Jiang, C., Yang, Y., Chen, X., Liao, J., Song, W., Zhang, X. (2021). A new-dynamic adaptive data rate algorithm of LoRaWAN in harsh environment. IEEE Internet of Things Journal, 9(11): 8989-9001. https://doi.org/10.1109/JIOT.2021.3118051

[3] Georgiou, O., Raza, U. (2017). Low power wide area network analysis: Can LoRa scale? IEEE Wireless Communications Letters, 6(2): 162-165. https://doi.org/10.1109/LWC.2016.2647247

[4] Bor, M.C., Roedig, U., Voigt, T., Alonso, J.M. (2016). Do LoRa low-power wide-area networks scale? In Proceedings of the 19th ACM International Conference on Modeling, Analysis and Simulation of Wireless and Mobile Systems, Malta, pp. 59-67. https://doi.org/10.1145/2988287.2989163

[5] Adelantado, F., Vilajosana, X., Tuset-Peiro, P., Martinez, B., Melia-Segui, J., Watteyne, T. (2017). Understanding the limits of LoRaWAN. IEEE Communications Magazine, 55(9): 34-40. https://doi.org/10.1109/MCOM.2017.1600613

[6] Vangelista, L. (2017). Frequency shift chirp modulation: The LoRa modulation. IEEE Signal Processing Letters, 24(12): 1818-1821. https://doi.org/10.1109/LSP.2017.2762960

[7] Augustin, A., Yi, J., Clausen, T., Townsley, W.M. (2016). A study of LoRa: Long range & low power networks for the internet of things. Sensors, 16(9): 1466. https://doi.org/10.3390/s16091466

[8] Burghal, D., Li, Y., Madadi, P., Hu, Y., Jeon, J., Cho, J. (2023). Enhanced AI-based CSI prediction solutions for massive MIMO in 5G and 6G systems. IEEE Access, 11: 117810-117825. https://doi.org/10.1109/ACCESS.2023.3324399

[9] Jiang, Y., Wang, M., Wang, X. (2023). A efficient adaptive data rate algorithm in LoRaWAN networks: K-ADR. In 2023 24st Asia-Pacific Network Operations and Management Symposium (APNOMS), Sejong, Korea, pp. 183-188. https://ieeexplore.ieee.org/abstract/document/10258176.

[10] He, J.W. (2024). An optimized ADR algorithm for LoRa network based on EWMA. In 2024 3rd International Conference on Artificial Intelligence, Internet of Things and Cloud Computing Technology (AIoTC), Wuhan, China, pp. 235-239. https://doi.org/10.1109/AIoTC63215.2024.10748331

[11] Slabicki, M., Premsankar, G., Di Francesco, M. (2018). Adaptive configuration of LoRa networks for dense IoT deployments. In NOMS 2018-2018 IEEE/IFIP Network Operations and Management Symposium, Taipei, Taiwan, pp. 1-9.

https://doi.org/10.1109/NOMS.2018.8406255
[12] Li, S., Raza, U., Khan, A. (2018). How agile is the adaptive data rate mechanism of LoRaWAN? In 2018 IEEE Global Communications Conference (GLOBECOM), pp. 206-212. https://doi.org/10.1109/GLOCOM.2018.8647469
[13] Babaki, J., Rasti, M., Taskou, S.K. (2020). Improved configuration of transmission variables for LoRaWAN in high-noise channels. In 2020 28th Iranian Conference on Electrical Engineering (ICEE), Tabriz, Iran, pp. 1-6. https://doi.org/10.1109/ICEE50131.2020.9260713
[14] Farhad, A., Kim, D.H., Subedi, S., Pyun, J.Y. (2020). Enhanced LoRaWAN adaptive data rate for mobile Internet of Things devices. Sensors, 20(22): 6466. https://doi.org/10.3390/s20226466
[15] Serati, R., Teymuri, B., Anagnostopoulos, N.A., Rasti, M. (2022). ADR-lite: A low-complexity adaptive data rate scheme for the LoRa network. In 2022 18th International Conference on Wireless and Mobile Computing, Networking and Communications (WiMob), Thessaloniki, Greece, pp. 296-301. https://doi.org/10.1109/WiMob55322.2022.9941614
[16] Fedullo, T., Morato, A., Tramarin, F., Bellagente, P., Ferrari, P., Sisinni, E. (2021). Adaptive LoRaWAN transmission exploiting reinforcement learning: The industrial case. In 2021 IEEE International Workshop on Metrology for Industry 4.0 & IoT (MetroInd4. 0&IoT), Rome, Italy, pp. 671-676. https://doi.org/10.1109/MetroInd4.0IoT51437.2021.9488498
[17] de Jesus, G.G.M., Souza, R.D., Montez, C., Hoeller, A. (2020). LoRaWAN adaptive data rate with flexible link margin. IEEE Internet of Things Journal, 8(7): 6053-6061. https://doi.org/10.1109/JIOT.2020.3033797
[18] Wang, H., Zhang, X., Liao, J., Zhang, Y., Li, H. (2024). An improved adaptive data rate algorithm of LoRaWAN for agricultural mobile sensor nodes. Computers and Electronics in Agriculture, 219: 108773. https://doi.org/10.1016/j.compag.2024.108773
[19] Bonilla, V., Campoverde, B., Yoo, S.G. (2023). A systematic literature review of LoRaWAN: Sensors and applications. Sensors, 23(20): 8440. https://doi.org/10.3390/s23208440
[20] Navarro-Ortiz, J., Chinchilla-Romero, N., Delgado-Ferro, F., Ramos-Munoz, J.J. (2022). A LoRaWAN network architecture with MQTT2MULTICAST. Electronics, 11(6): 872. https://doi.org/10.3390/electronics11060872
[21] Semtech LoRa Technology Overview \textbar Semtech. https://www.semtech.com/lora, accessed on Oct. 14, 2023.
[22] Babaki, J., Rasti, M., Aslani, R. (2020). Dynamic spreading factor and power allocation of LoRa networks for dense IoT deployments. In 2020 IEEE 31st Annual International Symposium on Personal, Indoor and Mobile Radio Communications, pp. 1-6. https://doi.org/10.1109/PIMRC48278.2020.9217283
[23] Al-Gumaei, Y.A., Aslam, N., Aljaidi, M., Al-Saman, A., Alsarhan, A., Ashyap, A.Y. (2022). A novel approach to improve the adaptive-data-rate scheme for IoT LoRaWAN. Electronics, 11(21): 3521. https://doi.org/10.3390/electronics11213521
[24] Farhad, A., Kwon, G.R., Pyun, J.Y. (2023). Mobility adaptive data rate based on Kalman filter for LoRa-empowered IoT applications. In 2023 IEEE 20th Consumer Communications & Networking Conference (CCNC), Las Vegas, NV, USA, pp. 321-324. https://doi.org/10.1109/CCNC51644.2023.10060330
[25] Kufakunesu, R., Hancke, G., Abu-Mahfouz, A. (2022). A fuzzy-logic based adaptive data rate scheme for energy-efficient LoRaWAN communication. Journal of Sensor and Actuator Networks, 11(4): 65. https://doi.org/10.3390/jsan11040065